Available online at www.sciencedirect.com
SCIENCE DIRECT®
Catalysis Today 98 (2004) 403–412
CATALYSIS TODAY
www.elsevier.com/locate/cattod

Ignition analysis of wall-flow monolith diesel particulate filters

Haishan Zheng, Jason M. Keith*

Department of Chemical Engineering, Michigan Technological University, Houghton, MI 49931, USA

Available online 29 September 2004

Abstract

During regeneration the diesel particulate filter (DPF) is a dynamic system whose trajectory depends on various parameters, especially the inlet gas temperature. Parametric sensitivity signifies large changes in the DPF trajectory induced by small changes in parameters across threshold values. This is a form of critical behavior and can lead to ignition conditions, which is necessary for complete regeneration. In this paper a transient one-phase model is used to derive analytical ignition criteria for a wall-flow monolith diesel particulate filter, which defines the ignition boundaries. The ignition criterion is a function of three parameters: α (a ratio of reaction time to convection time), B (a ratio of adiabatic temperature rise to the characteristic temperature for reaction), and γ (a ratio of total heat capacities of the soot bed to the substrate wall) and is given by $\alpha/\beta < e$ when reactant consumption is unimportant ($B \gg 10$) and $\alpha/\beta + f(\gamma)B^{-g(\gamma)} < e$ when reactant consumption is important. For most practical cases of the DPF $f(\gamma) = 6.0074$ and $g(\gamma) = 0.6411$. The validity of the ignition criteria is verified by numerical simulations using the transient one-phase model. The effect of several parameters, i.e., the wall thickness, the total filtration area, the initial loading, the gas flow rate, the oxygen feed concentration, and on the critical inlet gas temperature are also discussed. It is shown that a thin channel wall, a high total filtration area, a high initial loading, a low gas flow rate and a high oxygen feed concentration are desirable for an efficient regeneration.

Keywords: Ignition; Thermal regeneration; Diesel particulate filter; Wall-flow monolith filter

1. Introduction

Diesel particulate filters (DPF) are now widely used in diesel particulate emission control, standards for which have become tighter year by year on a worldwide basis. One of the most promising devices, the wall-flow monolithic filter, consists of many parallel channels, which are alternately plugged at either end in order to force the exhaust gases through the porous ceramic walls. The particulates are deposited on the inside wall of the inlet channel to form a thin, porous soot bed. Once a sufficient mass of particulates is collected, it is burned off to regenerate the filter by heating the exhaust gas with either an electric heater or a diesel oxidation catalyst (DOC) reactor. Controlling the exhaust gas temperature at the inlet of the filter is a critical area of the diesel exhaust system design, since insufficient heating cannot fully combust the particulates and excessive heating can reduce engine fuel economy. In addition, overheating results in a very high temperature peak, which can cause a structural failure of the filter. Therefore, it is important to be able to study the minimum inlet gas temperature beyond which the particulates are completely combusted.

Due to the highly exothermic nature of the soot oxidation, the regeneration process in the DPF has similarity with combustive reactions. There exists a clear, sharp temperature rise when the solid temperature is heated beyond an ignition temperature. Many efforts have been devoted to study such an ignition temperature for soot oxidation. The temperature at which soot ignites is defined differently by different authors and for different equipment.

In thermogravimetric analysis (TGA) temperature ramping tests, Lahaye et al. defined the ignition temperature as the intercept on the temperature axis of the linear part of the weight loss versus temperature curve [1]. They found that uncatalysed soot ignites at temperatures above 500 °C. McCabe and Sinkevitch studied the ignition of soot beds [2]. In the reactor to visualize and video regeneration (RVVR) system, they heated soot beds by radiation and found that, without catalyst, the ignition temperature of soot, which is

* Corresponding author. Tel.: +1 906 487 2106; fax: +1 906 487 3213.
E-mail address: jmkeith@mtu.edu (J.M. Keith).

0920-5861/$ – see front matter © 2004 Elsevier B.V. All rights reserved.
doi:10.1016/j.cattod.2004.08.008

Nomenclature

A	filtration area, 1.63 (m^2)
B	a key characteristic temperature ratio
C_{pg}	heat capacity of gas, 1.09×10^3 (J/kg K)
C_{p1}	heat capacity of deposit layer, 1.51×10^3 (J/kg K)
C_{p2}	heat capacity of porous ceramic, 1.11×10^3 (J/kg K)
E/R	activation energy/gas constant, 1.8×10^4 (K)
F	mass flow rate of inlet gas, 0.0523 (kg/s)
ΔH	heat of reaction, -3.93×10^8 (J/kg mol)
k_j	rate coefficient for the reaction in region j (m/s)
k	rate constant, 596 (m/s K)
M_a	molecular weight of gaseous mixture, 29.0 (kg/kg mol)
M_c	atomic weight of deposit, 12.0 (kg/kg mol)
m	initial mass of deposit, 20 (g)
P	pressure, 101 (kPa)
R	gas constant, 8.31 (m^3 kPa/kg mol K)
S_1	specific area of deposit layer, 5.5×10^7 (m^{-1})
T	temperature in the filter (K)
T_b	initial temperature, 606 (K)
T_i	inlet temperature (K)
ΔT_{ad}	adiabatic temperature rise (K)
t	time (s)
t_C	the characteristic time for thermal convection
t_R	the characteristic time for reaction
w	thickness of the particulate deposit layer (m)
w_b	initial thickness of the particulate deposit layer (m)
w_s	thickness of wall of monolith channel, 4.32×10^{-4} (m)
x	distance (m)
y	mole fraction of oxygen
$y_i(t)$	mole fraction of oxygen at the inlet
Z	the dimensionless deposit thickness

Greek letters

α	a key timescale ratio
γ	a ratio of the total heat capacity of soot bed over the total heat capacity of substrate wall
λ_1	bulk thermal conductivity of deposit layer, 0.84 (W/m K)
λ_2	bulk thermal conductivity of porous ceramic, 1.1 (W/m K)
θ	dimensionless temperature
ρ	density of gas (kg/m^3)
ρ_1	bulk density of deposit layer, 5.5×10^2 (kg/m^3)
ρ_2	bulk density of porous ceramic, 1.4×10^3 (kg/m^3)
τ	dimensionless time

Subscripts

i	inlet condition
j = 1,2	indicating particulate region (j = 1) and ceramic region (j = 2)

defined as the temperature at which the irradiated part of the bed sustains a rapid temperature rise and begins to glow, is above 600 °C. They modeled this behavior by assuming that the bed soot is isothermal and the sensible heat of the gas phase is negligible, compared to the solid. By assuming that ignition occurs when the thermal accumulation term is equal to the sum of the convective and reactive terms, the model successfully predicted ignition temperatures over a range of experimental conditions. Stanmore et al. extended this model developed using measured kinetics for catalysed and uncatalysed soot and predicted the differences in their ignition temperature [3].

It is worth stressing that these ignition temperatures were measured by directly ramping the temperature of the soot bed with a linear heating rate. The results do not reflect the conditions during the DPF regeneration when the exhaust gas flow is forced through the soot bed. In the case of the DPF, the soot bed is initially heated by the exhaust gas flow. After the solid temperature exceeds the inlet gas temperature, the soot bed is only self-heated by reaction heat released by oxidation of soot, and the exhaust gas cools the soot bed. Zheng and Keith showed that for inlet gas temperatures below a critical value, which is lower than the ignition temperature, the system cannot reach the ignition temperature and fails to ignite [4]. The minimum value of the inlet gas temperature required for ignition, which will be referred to as the critical inlet gas temperature, strongly depends on operating conditions such as the flow rate and oxygen concentration but also on the size and material properties of the DPF. Therefore, it is more important to be able to predict this critical inlet gas temperature of a DPF system than the ignition temperature of soot oxidation in order to optimize the design of the regeneration system and improve the fuel economy. Such a critical inlet gas temperature can be obtained from the ignition criteria for the DPF. Extensive studies exist in the literature on the derivation of ignition criteria for packed-beds and catalytic converters [5–8]. However, a derivation of the ignition criteria for the DPF has not been reported.

In this paper we present analytical ignition criteria for the wall-flow monolithic DPF, which can be used to predict the critical inlet gas temperature. The derivation of ignition criteria is based on the transient one-phase model of Bissett and Shadman [9] with an assumption of constant oxygen concentration through the soot layer before ignition. This is a key assumption, which leads to slightly conservative criteria but simplifies the mathematical model to allow analytical ignition criteria to be derived. First, we present an analytical ignition criterion with the application of Semenov theory, which neglects reactant consumption. We then use the ignition theory of Adler and Enig [10] to derive an ignition criterion, which accounts for reactant assumption. These criteria are subsequently validated with numerical simulations using Bissett and Shadman's model. Finally, we discuss the influence of different parameters on the critical inlet gas temperature of the DPF.

2. Mathematical model for wall-flow monolith DPF

Bissett and Shadman developed a transient one-phase model of the regeneration process in the wall-flow monolithic filter [9]. The model developed in their article considers that the gas flows through two layers: the particle deposit, which shrinks with time during regeneration, and the porous channel wall, which remains unchanged (Fig. 1). This model assumes a uniform flow distribution at the monolith face and adiabatic operation of the monolith filter. Under these assumptions, all channels behave the same, thus allowing consideration of only one channel instead of all channels. The following assumptions are also made: (1) neglecting the change in the internal structure of the deposit during regeneration, (2) neglecting addition of particles to the deposit during regeneration, (3) neglecting all variations in the directions perpendicular to the x-direction, (4) neglecting axial diffusion of mass and heat in the gas phase, and (5) neglecting temperature gradients between the gas and solid phase except at the inlet face of the deposit layer, $x = -w$.

The assumption of equal solid and gas temperatures is sufficiently valid over the range of conditions encountered during regeneration in the DPF. Under typical conditions, the pore diameters of the substrate wall are about 10 μm [11] and that of the particulate layer are about 0.1 μm [12]. The small pore size significantly reduces the interphase transport time, which is several orders of magnitude smaller than typical the residence time. Therefore, the pseudo-homogeneous model is valid, and the difference between the gas temperature and the solid phase temperature can be safely omitted.

With the above assumptions, the model equations are given by

$$\frac{\partial}{\partial x}(\rho v y) = -s_j k_j \rho y, \quad j = 1\ (\text{particulate}),\ 2\ (\text{ceramic}) \tag{1}$$

$$\rho_j C_{pj} \frac{\partial T}{\partial t} = s_j \left(-\frac{\Delta H}{M_a}\right) k_j \rho y + \frac{\partial}{\partial x}\left(\lambda_j \frac{\partial T}{\partial x}\right) - \rho v C_{pg} \frac{\partial T}{\partial x} \tag{2}$$

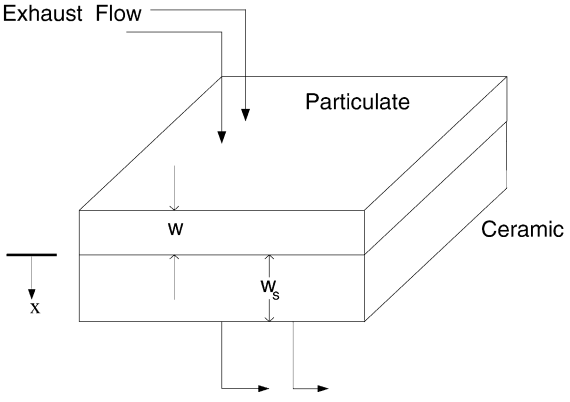

Fig. 1. Model geometry for a section of the filtration area.

$$\rho_1 \frac{\mathrm{d}w}{\mathrm{d}t} = \left(\frac{M_c}{M_a}\right)\left[\frac{F(t)}{A}\right]\left[y|_{x=0} - y|_{x=-w}\right] \tag{3}$$

where ρ is the gas density, v the gas velocity, s_j the specific area of the region j, k_j the rate coefficient for the reaction in region j, y the oxygen mole fraction, the thickness of the deposit layer, M_c the atomic weight of the deposit and M_a the molecular weight of the exhaust gas, $F(t)$ is the mass flow rate of the inlet gas.

The initial conditions for this system are prescribed as:

$$T(x, t = 0) = T_b, \qquad w(t = 0) = w_b \tag{4}$$

and boundary conditions are

$$y = y_i(t), \qquad \text{at } x = -w \tag{5}$$

$$\lambda_1 \frac{\partial T}{\partial x} = \rho v C_{pg}[T - T_i(t)], \quad \text{at } x = -w \tag{6}$$

$$\frac{\partial T}{\partial x} = 0, \quad \text{at } x = w_s \tag{7}$$

where $y_i(t)$ is the mole fraction of oxygen at the inlet, $T_i(t)$ the inlet temperature, and w_s the thickness of the monolith channel wall.

Using a perturbation expansion in T, y and w, these equations can be solved to give two ODE equations [9]:

$$\frac{\mathrm{d}T}{\mathrm{d}t} = \frac{1}{\rho_1 C_{p1} w + \rho_2 C_{p2} w_s} \times \left\{ \frac{(-\Delta H) F y}{M_a A}\left[1 - \exp\left(-\frac{s_1 A P M_a w k}{RF} \exp\left(-\frac{E}{RT}\right)\right)\right] - \frac{F C_{pg}}{A}(T - T_i)\right\} \tag{8a}$$

$$\frac{\mathrm{d}w}{\mathrm{d}t} = -\frac{M_c F y}{M_a \rho_1 A}\left[1 - \exp\left(-\frac{s_1 A P M_a w k}{RF} \exp\left(-\frac{E}{RT}\right)\right)\right] \tag{8b}$$

where A is the filtration area.

It should be noted that spatially uniform temperatures are not assumed initially, but that they are derived from the fact that the leading-order term of the perturbation expansion of T is independent of x. This assumption of spatially uniform temperatures is reasonable because the thermal Peclet number is small. The conduction is dominant in the thin x-direction. Although the assumption of spatially uniform temperatures simplifies the model considerably, the exponential in the reaction rate expressions makes it impossible to derive analytical ignition criteria. In next section, we simplify the model.

3. Simplified DPF model

For the case of spatially uniform temperatures, Eq. (1) can be integrated to give the oxygen concentration profile

through the soot layer:

$$y = y_i \exp\left(-\frac{s_1 A P M_a k_1}{RTF}(x+w)\right), \quad x \le 0 \tag{9}$$

where $k_1 = kT\,e^{(-E/RT)}$.

Calculation of Eq. (9) indicates that the oxygen concentration is almost constant through the soot layer before ignition due to the slow reaction kinetics. Therefore, we can further simplify the model by assuming a constant oxygen concentration through the soot layer before ignition. This is a key assumption, which simplifies the reaction term considerably and enable us to derive analytical ignition criteria.

It should be pointed out that the assumption of constant oxygen concentration throughout the deposit layer is not true after ignition. After ignition, the reaction is so quick that nearly all of the oxygen is consumed in the top layer of the soot bed. The reaction is limited by the rate of oxygen transport to the soot layer, which is proportional to the flow rate and oxygen concentration. In this case, the assumption of constant oxygen concentration through the soot layer overestimates the reaction rate. Although this assumption leads to a quantitative error after ignition, it is usually satisfied before ignition over most operating conditions and therefore introduces little error in the derivation of ignition criteria. Therefore, we can safely use this simple model to derive analytical ignition criteria for the DPF.

Thus, Eq. (1) can be neglected, and Eq. (3) becomes

$$\rho_1 \frac{dw}{dt} = -\frac{M_c s_1 P y w k}{R} \exp\left(-\frac{E}{RT}\right) \tag{10}$$

Integration of Eq. (2) from to w_s gives

$$(\rho_1 A w C_{p1} + \rho_2 A w_s C_{ps}) \frac{dT}{dt} = \frac{(-\Delta H) s_1 P y w A k}{R} \exp\left(-\frac{E}{RT}\right) - F C_{pg}(T - T_i) \tag{11}$$

Using the Frank-Kamenetskii approximation, the reaction kinetics are expanded about T_i,

$$\exp\left(-\frac{E}{RT}\right) \sim \exp\left(-\frac{E}{RT_i}\right)\left(\exp\ \frac{E}{RT_i^2}(T - T_i)\right) \tag{12}$$

It is conventional to cast the model equations in dimensionless form, such that

$$\frac{d\theta}{d\tau} = \frac{BZ\,e^{\theta} - \alpha\theta}{1 + \gamma Z} \tag{13a}$$

$$\frac{dZ}{d\tau} = -Z\,e^{\theta} \tag{13b}$$

where $Z = w/w_b$, is a dimensionless deposit thickness, $\theta = (E/RT_i^2)(T - T_i)$, is a dimensionless temperature, $\tau = t/t_R$, is a dimensionless time, $t_C = \rho_2 C_{p2} A w_s / F C_{pg}$, is the characteristic time for thermal convection, $t_R = \rho_1 R / M_C P y s_1 k \exp(-E/RT_i)$, is the characteristic time for reaction, $\gamma = \rho_1 C_{p1} w_b / \rho_2 C_{p2} w_s$, is a ratio of the total heat capacity of the soot bed over the total heat capacity of the substrate wall, $\alpha = t_R/t_C$, is the ratio of reaction and convection times, $\Delta T_{ad} = (-\Delta H) w_b \rho_1 / M_c \rho_2 w_s C_{p2}$, is the adiabatic temperature rise, and $B = (E/RT_i^2)\Delta T_{ad}$, is a key characteristic temperature ratio, the adiabatic temperature rise divided by a characteristic temperature for reaction to occur, with initial conditions

$$\theta(\tau = 0) = 0, \qquad Z(\tau = 0) = 1$$

It is worthwhile to point out that at the beginning of regeneration the temperature of the solid phase is usually lower than the inlet gas temperature. However, the reaction rate is very low at this stage, and deposit consumption is negligible. Therefore, we can ignore the behavior of the system before the solid phase reaches equilibrium with the exhaust gas, and treat the regeneration as starting from an equilibrium state.

4. Analytical ignition criteria

In this section, we derive ignition criteria for the DPF and validate them by comparison with the full model. We consider two cases: with and without reactant consumption.

4.1. Neglecting reactant consumption

When reactant consumption is ignored, Eq. (13b) disappears since $Z = 1$ is constant. The roots of the steady state $d\theta/d\tau = 0$ can be obtained from

$$\frac{\alpha}{B} = \frac{e^{\theta s}}{\theta_s} \tag{14}$$

Regarding this as an equation for θ_s as a function of α/B, Fig. 2 shows that there is no solution for Eq. (14) if $\alpha/B < (\alpha/B)_C$, which means that the rate of heat generation is always greater than the rate of heat loss, and $\theta(\tau)$ monotonically increases to infinity which means ignition occurs. In the case of $\alpha/B > (\alpha/B)_C$, there are two solutions to Eq. (14): θ_{st} (steady state point) and θ_{ig} (ignition point). Since the DPF is only heated by the exhaust gas flow, the DPF can only reach steady state at $\theta = \theta_{st}$ with no ignition during the regeneration process. Therefore, $(\alpha/B)_C$ defines the conditions for the critical state. Using $d^2\theta/d\tau^2 = 0$ at the critical point gives

$$e^{\theta} = \frac{\alpha}{B} \tag{15}$$

Substitution of Eq. (15) into Eq. (14) gives the critical condition $(\alpha/B)_C = e$ at the critical state $\theta_c = 1$.

To obtain ignition during the regeneration of the DPF, the operating conditions must satisfy the following condition

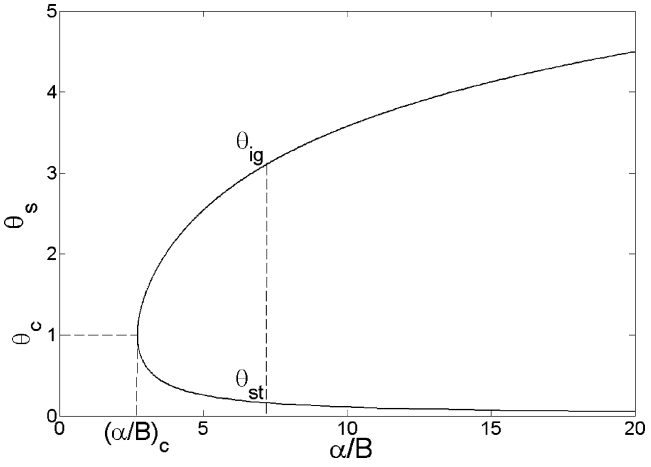

Fig. 2. Variation of stationary temperature θ_s with the parameter α/B.

that is given by $\alpha/B < (\alpha/B)_C$

$$\frac{FC_{pg}R^2T_i^2\exp(E/RT_i)}{(-\Delta H)s_1Pyw_bAEk} < 2.7183 \tag{16}$$

Physically this suggests small reaction time to convection time ratio (i.e., low gas flow rates for a small α parameter) and a large adiabatic temperature rise (thick initial deposit for a large B parameter).

4.2. Accounting for reactant consumption

We now consider the effect of reactant consumption on DPF ignition criteria. Clearly, when reactant consumption is taken into account, a steady state does not exist during regeneration. The solid temperature will reach a maximum due to self-heating, and then must decay to the temperature of the exhaust gas due to soot depletion. Therefore, the stationary Semenov theory is not suitable for cases accounting for reactant consumption. Eq. (13) is similar to the model of a batch reactor with a uniform temperature and concentration, for which there exist many theories on the criticality of ignition. Rice et al. defined criticality with reactant consumption as the attainment of an inflection point in the $\theta - \tau$ plane before the solid temperature reaches the maximum [13]. Equivalently, the criticality is at the point where $d\theta/d\tau > 0$, $d^2\theta/d\tau^2 = 0$, and $d^3\theta/d\tau^3 = 0$. Adler and Enig defined criticality as that which possesses a single inflection point in the $\theta - Z$ trajectory instead of the $\theta - \tau$ trajectory before θ reaches a maximum [10]. This critical state can be described by

$$\frac{d\theta}{dZ} < 0, \qquad \frac{d^2\theta}{dZ^2} = 0, \qquad \text{and} \qquad \frac{d^3\theta}{dZ^3} = 0 \tag{17}$$

The critical states in these two plane coincide only when $B = \infty$, which means negligible reactant consumption. Shouman and El-Sayed proved that the critical state in the $\theta - \tau$ plane is always subcritical (no ignition) in the $\theta - Z$ plane, and the critical state in the $\theta - Z$ plane is always supercritical (ignition) in the $\theta - \tau$ plane [14]. Therefore, we use Adler and Enig's theory to derive the critical ignition point in the DPF, because it guarantees finding the correct value.

Combining Eq. (13) to eliminate τ gives

$$\frac{d\theta}{dZ} = \frac{1}{1+\gamma Z}\left(\frac{\alpha\theta e^{-\theta}}{Z} - B\right) \tag{18}$$

with the initial condition of $Z = 1$ at $\theta = 0$.

Differentiating Eq. (18) with respect to Z gives

$$\frac{d^2\theta}{dZ^2} = \frac{1}{1+\gamma Z}\left\{\left[\frac{\alpha(1-\theta)e^{-\theta}}{Z} - \gamma\right]\frac{d\theta}{dZ} - \frac{\alpha\theta e^{-\theta}}{Z^2}\right\} \tag{19}$$

Furthermore, differentiation of Eq. (19) with respect to Z gives

$$\frac{d^3\theta}{dZ^3} = \frac{1}{1+\gamma Z}\left\{\frac{2\alpha\theta e^{-\theta}}{Z^3} + \left[\frac{\alpha(1-\theta)e^{-\theta}}{Z} - 2\gamma\right]\frac{d^2\theta}{dZ^2} + \frac{2\alpha(\theta-1)e^{-\theta}}{Z^2}\frac{d\theta}{dz} + \frac{\alpha(\theta-2)e^{-\theta}}{Z}\left(\frac{d\theta}{dZ}\right)^2\right\} \tag{20}$$

with $d^2\theta/dZ^2 = 0$ and $d^3\theta/dZ^3 = 0$, we obtain two equations,

$$B\gamma Z^2 - (2\gamma\theta + B(1-\theta))\alpha e^{-\theta}Z + (\alpha(1-\theta)e^{-\theta} - 1)\alpha\theta e^{-\theta} = 0 \tag{21a}$$

$$2\gamma^2Z^2 - 2\gamma\alpha(1-\theta)e^{-\theta}Z + (\theta-2)\alpha^2\theta e^{-2\theta} = 0 \tag{21b}$$

The roots $\theta_c(\gamma, \alpha, B)$ and $Z_c(\gamma, \alpha, B)$ of Eq. (21) define the critical trajectory. The parameters α_c and B_c that produce the critical trajectory are the critical parameters. They can be obtained by numerically integrating Eq. (18) and adjusting the values of α and B via the shooting method to satisfy Eq. (21).

The value of B for the DPF is in the range between 20 and 50. Although not true for all values of B, over this important range the critical value of α and B are related to each other by the relationship:

$$\frac{\alpha_c}{B_c} = e - f(\gamma)B_c^{-g(\gamma)} \tag{22}$$

where $f(\gamma)$ and $g(\gamma)$ are function of γ, the ratio of the total heat capacity of the soot bed to the total heat capacity of the substrate wall. This is shown in Fig. 3, which shows that a plot of $e - \alpha_c/B_c$ as a function of B_c is linear on a logarithmic scale.

Writing Eq. (22) in dimensional terms gives the ignition criterion of the DPF when reactant consumption is accounted for

$$\frac{FC_{pg}R^2T_i^2\exp(E/RT_i)}{(-\Delta H)s_1Pyw_bAkE} + f(\gamma)\times\left(\frac{(-\Delta H)w_b\rho_1E}{M_c\rho_2w_sC_{p2}RT_i^2}\right)^{-g(\gamma)} < 2.7183 \tag{23}$$

when γ increases from 0 to 1, $f(\gamma)$ increases from 6.0074 to 7.8154, and $g(\gamma)$ decreases from 0.6411 to 0.6080, as shown

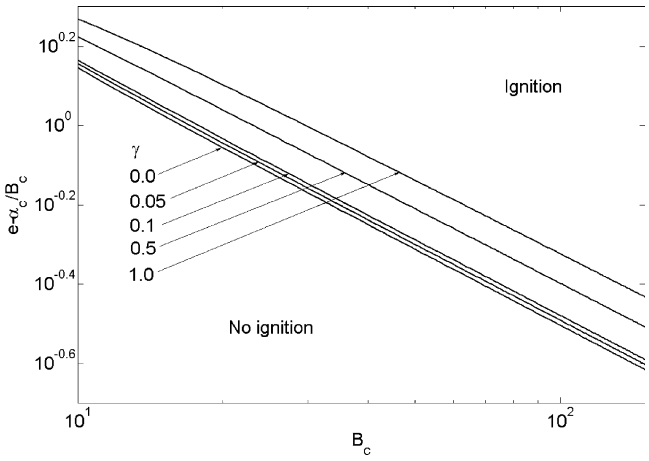

Fig. 3. Plots of $e - \alpha_c/B_c$ vs. B_c for different γ.

in Table 1. It can be seen that γ has little effect on the value of $g(\gamma)$, which only decreases 5% as γ increases from 0 to 1. The changes of both $f(\gamma)$ and $g(\gamma)$ are very small for $\gamma < 0.1$.

When $\gamma = 0$, Eq. (21) gives the solution as

$$\theta_c = 2, \quad \text{and} \quad Z_c = \frac{2\alpha\, e^{-2} + 2}{B} \tag{24}$$

which are classical results reported by Adler and Enig for thermal explosions. Fig. 4 shows the effect of γ on θ_c and Z_c. As expected, the value of θ_c and Z_c decreases as γ increases. The reason is that the system can be more easily ignited when the amount of deposit increases. As illustrated in Fig. 4, the effect of γ is negligible for $\gamma < 0.1$. In the case of the DPF, γ is usually small and <0.1. The most interesting fact about the DPF is that B increases as γ increases. For the case of γ larger than 0.1, the value of B will become very large, when the effect of γ is still very small. Therefore, we can neglect γ for the DPF. This can simply the ignition criterion (Eq. (23)) to give

$$\frac{FC_{pg}R^2T_i^2\exp(E/RT_i)}{(-\Delta H)s_1 P y w_b A k E} + 6.0074 \times \left(\frac{(-\Delta H)w_b\rho_1 E}{M_c\rho_2 w_s C_{p2} R T_i^2}\right)^{-0.6411} < 2.7183 \tag{25}$$

It should be noted that for the system with small values of B, especially around 10, and γ larger than 0.5, the value of $f(\gamma)$ and $g(\gamma)$ will significantly affect the ignition criterion. In this case, Eq. (23) should be used for ignition criteria, and the value of $f(\gamma)$ and $g(\gamma)$ should be replaced by their value from Table 1.

Table 1
The value of $f(\gamma)$ and $g(\gamma)$ for different γ

γ	$f(\gamma)$	$g(\gamma)$
0.0	6.0074	0.6411
0.001	6.0099	0.6411
0.01	6.0333	0.6407
0.05	6.1362	0.6393
0.1	6.2601	0.6375
0.5	7.0915	0.6241
1.0	7.8154	0.6080

It should also be noted that the first term in the left side of Eq. (23) is the ignition criterion with no reactant consumption. It depends on operating conditions such as the gas flow rate, oxygen concentration, and especially inlet gas temperature but not on the physical properties of the DPF wall. This term decreases quickly with increasing inlet gas temperature. The second term accounts for the reactant consumption and is almost proportional to the inlet gas temperature. It strongly depends on the physical properties of the DPF wall. Both the first and second term will be affected by changing the initial soot loading. The value of $f(\gamma)$ and $g(\gamma)$ have little effect on the ignition criterion when the value of B is large ($B \gg 10$). In this limit we can use the value for $\gamma = 0$.

4.3. Comparison with the full model

In this section, we compare the critical inlet gas temperature calculated from the above analytical ignition criteria with those obtained from the ''full model'' using the parameters listed in Bissett and Shadman's paper [9]. For such comparisons, we assume that the inlet conditions are independent of time. Before comparison, we first define how the critical inlet gas temperature is obtained for Bissett and Shadman's model. We numerically integrate Eqs. (8a) and (8b) for different inlet gas temperatures, and draw a graph of the maximum solid temperature versus the inlet gas temperature. The critical inlet gas temperature is the inlet gas temperature at which a ''jump'' of the maximum solid temperature appears. Eqs. (8a) and (8b) are first order with known initial conditions. They were directly integrated by using a forward finite difference method. An absolute error tolerance of 10^{-8} was imposed to accommodate the deposit thickness w when it approaches 0.

Fig. 5 presents the plots of the critical inlet gas temperature versus the gas flow rate. It can be seen that the agreement between the full model (solid curve) and the analytical ignition criterion with reactant consumption for γ = 0 (dashed curve) is excellent, within 2–4 °C. Using the original parameters of Bissett and Shadman, the actual value of γ is 0.0276. However, we can use the $\gamma = 0$ case with little error because the effect of γ is very small. The analytical ignition criterion with no reactant consumption (using the original parameters of Bissett and Shadman, $B = 23.4$ for the inlet gas temperature of 679 K) predicts critical inlet temperatures that are 10–12 °C lower than that of the full model. It should be noted that the error (when reactant consumption is neglected) increases as B decreases. When B is around 10, the difference could be 20–30 °C. Therefore, Eq. (16) can only be used for the case $B \gg 10$ to provide a simple and quick way to calculate the critical inlet gas temperature.

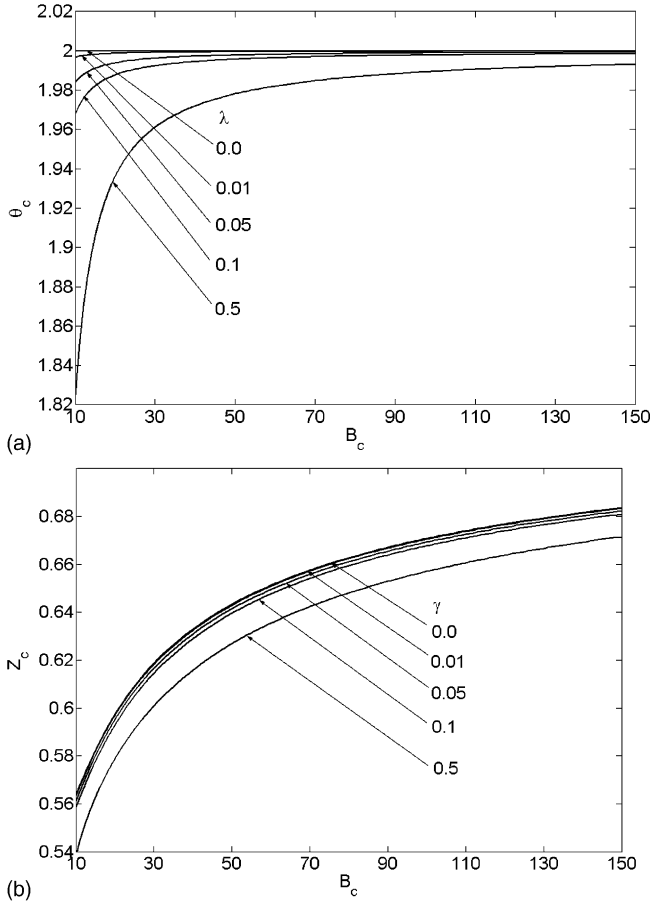

Fig. 4. (a) The critical state temperature θ_c for different critical parameters B_c and γ. The lines are also dependent on α_c. (b) The critical state deposit thickness Z_c for different critical parameters B_c and γ. The lines are also dependent of α_c.

5. Influence of various design and operating variables on ignition

A good DPF system requires a low pressure loss, a high PM filtration efficiency, and a good fuel economy. To obtain a good fuel economy in an optimum design, the effect of various design variables on ignition, especially on the critical inlet gas temperature, should be analyzed. In this section we analyze these effects by using the above ignition criterion accounting for reactant consumption.

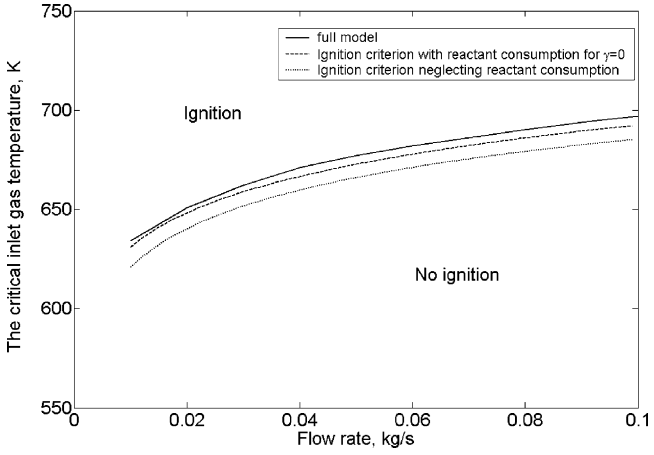

Fig. 5. Model comparison of the critical inlet gas temperature for various flow rates.

The wall thickness w_s of the DPF is a critical design variable. Ogyu et al. reported that the reduction in wall thickness is effective in decreasing pressure loss without a loss of filtration efficiency [15]. From the above ignition criterion we can see that wall thickness also affects the critical inlet gas temperature required for ignition. It can be seen from the ignition criterion (Eq. (25)) that the reduction in wall thickness decreases the second term of the LHS of Eq. (25). The effects of variations of wall thickness on a critical inlet gas temperature are shown in Fig. 6. It shows that a critical inlet gas temperature required for ignition keep decreasing with decreasing wall thickness. When the wall thickness decreases from $2w_s$ to $0.5w_s$ the critical inlet gas temperatures decreases 8–12 °C. As the wall thickness decreases further, the benefit becomes small. From $0.5w_s$ to $0.1w_s$ the critical inlet gas temperature only decreases 2–4 °C. It can also been seen that the impact of decreasing the wall thickness on the critical inlet gas temperature is relatively higher at high flow rates than at low flow rates.

It is worthwhile to point out that the reduction of wall thickness increases both γ and B. Therefore, the difference

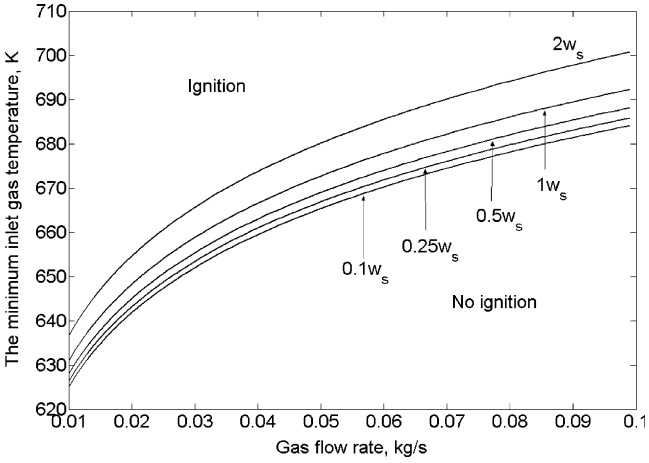

Fig. 6. The critical inlet gas temperature predicted by Eq. (25) for different wall thickness and gas flow rates.

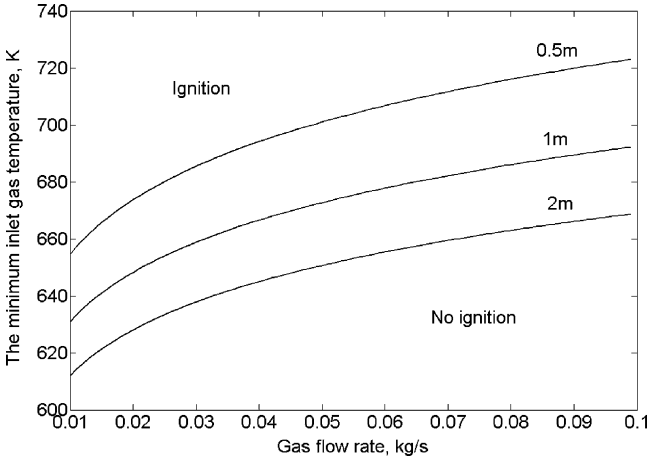

Fig. 8. The critical inlet gas temperature for various initial loading and gas flow rates.

between Eq. (23) (ignition criteria with reactant consumption and the full effect of γ) and 25 (ignition criteria with reactant consumption and $\gamma = 0$) in the predicted critical inlet gas temperature for both cases of $2w_s$ and $0.1w_s$ is only around 1 °C. We also note that if the wall thickness keeps decreasing, the critical inlet gas temperature predicted by Eq. (25) approaches those predicted by Eq. (16) (ignition criteria without reactant consumption) since the second term in Eq. (25) become negligible when B becomes very large.

The total filtration area A is another important design variable. Eq. (25) clearly shows that the change of total filtration area affects the first term in the LHS of Eq. (25). Fig. 7 shows the influence of the total filtration area on the critical inlet gas temperature for various gas flow rates. It can be seen that the decrease in the total filtration area with no change in initial thickness of the soot layer increases the critical inlet temperature. When the area increases from $0.5A$ to $2A$ the critical inlet gas temperature decreases around 40 °C. However, the big size of the DPF is not desirable because of a large space and high cost. Actually, the increase in area alone affects the critical inlet temperature by decreasing the gas velocity through the soot bed. Therefore, the effect of increasing the area is the same as that of decreasing the gas mass flow rate through the DPF. This can be seen clearly in Fig. 7 by the dashed lines.

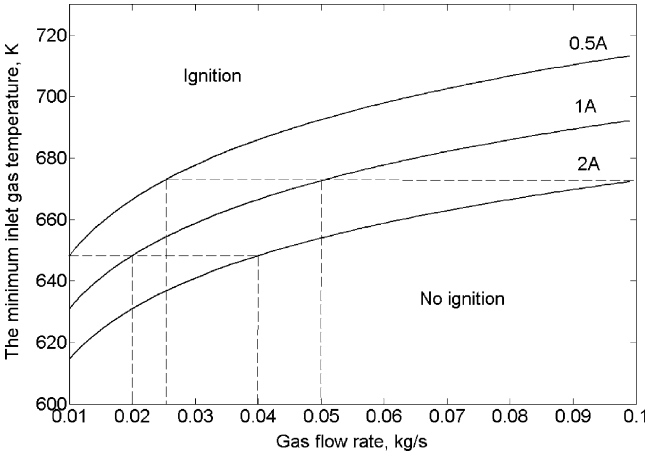

Fig. 7. The critical inlet gas temperature for various total filtration areas and gas flow rates.

The initial loading m or initial thickness of soot layer w_b is one design variable which can affect both terms in the LHS of Eq. (25). A high initial loading is desirable because it allows a low regeneration frequency. As shown in Fig. 8, the high loading also results in a lower critical inlet gas temperature. When the initial loading increases from 10 g ($0.5m$) to 40 g ($2m$), the critical inlet gas temperature decreases 35–50 °C, which greatly improves the fuel economy of the DPF. However, a higher initial loading also results in a high pressure drop in the DPF, which is not desirable. Therefore, there is a limit on increasing the initial loading, which is dictated by the operating requirements of the engine.

Several operating variables such as the gas mass flow rate F through the DPF and the oxygen feed concentration y also affect the critical inlet gas temperature. Zheng and Keith showed that a bypass design in the DPF system can improve the performance and fuel economy of regeneration by dividing the exhaust gas into two or three parts [4]. They pointed out that the critical inlet gas temperature decreases by increasing the number of channels in the DPF system. It can be seen here that changing the gas mass flow rate affects the first term of the LHS of Eq. (25). Figs. 5–8 all show that the reduction of the gas mass flow rate decreases the critical inlet gas temperature. This is because a decrease in the gas mass flow rate decreases the rate of heat removal.

The influence of the oxygen feed concentration y on the critical inlet gas temperature can also be analyzed with the help of Eq. (25). As illustrated in Fig. 9, increasing the oxygen mole fraction will greatly decrease the critical inlet gas temperature. It should be noted that when the mole fraction of oxygen is <0.1, the critical inlet gas temperature increases quickly with decreasing oxygen mole fraction.

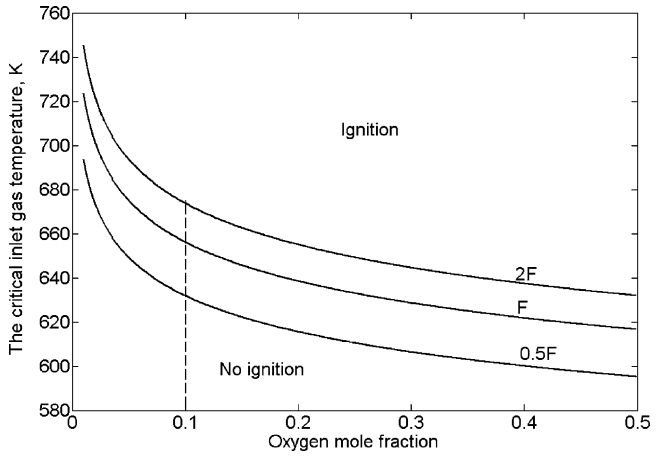

Fig. 9. The critical inlet gas temperature for different oxygen concentrations.

When the oxygen mole fraction is <0.01, the critical inlet gas temperature approaches infinity, which means no ignition during regeneration. It should also be pointed out that increasing the oxygen mole fraction also reduces the regeneration time which includes the time before ignition (reaction limited) and the time after ignition (mass transfer limited), which is proportional to the gas mass flow rate and oxygen mole fraction. Therefore, an oxygen mole fraction that is higher than 0.1 is required to obtain good fuel economy for the DPF because the filter can be regenerated with a low temperature feed.

6. Conclusions and discussion

A clear and sharp temperature rise during the DPF regeneration, which is similar to ignition phenomena in combustion reactions, has been reported by many authors. Many authors reported an ignition temperature in the range of 500–600 °C, which are measured by ramping the temperature of the soot bed with a linear heating rate. These results do not reflect the conditions of regeneration in the DPF. Zheng and Keith reported that there exists a critical inlet gas temperature required for ignition [4]. It is more important and useful to be able to predict the critical inlet gas temperature than the ignition temperature for soot oxidation. In this paper analytical ignition criteria for a wall-flow monolith DPF are presented by which a critical inlet gas temperature can be predicted. The ignition criteria are derived by simplifying Bissett and Shadman's model by assuming constant oxygen concentration through the soot layer.

Eq. (16) describes an ignition criterion without reactant consumption in the DPF. It reflects the effect of operating conditions such as the gas mass flow rate and oxygen concentration on the ignition criteria in the DPF. For the case of $B \gg 10$, Eq. (16) provides a simple and quick way to predict the critical inlet gas temperature required for ignition in the DPF. However, the error of Eq. (16) in predicting a critical inlet gas temperature increases as B decreases. It predicts a critical inlet gas temperature that is around 30 °C lower than that of the full model when B is around 10.

Eqs. (23) and (25) describe ignition criteria accounting for reactant consumption. The first term in the LHS of Eqs. (23) and (25) is the same as the ignition criterion without reactant consumption. The second term accounts for the effects of reactant consumption on ignition criterion. It clearly shows that changing wall substrate properties affects the ignition criterion.

One of the important new findings is that changing value of γ, which is the ratio of the total heat capacity of soot bed over the total heat capacity of substrate wall, also affects the ignition criterion. The temperature θ_c of the critical state equals 2 for $\gamma = 0$, which is the classical result reported by many authors. We show here that the temperature θ_c of the critical state decreases with increasing γ, and approaches 2 when B approaches infinity. It is also shown that the effect of changing γ on θ_c become small when the value of B increases. Therefore, the effect of γ on the ignition criterion can be neglected when $B \gg 10$ or $\gamma \ll 0.1$. Under these conditions, Eq. (25) should be used. However, the effect of λ on the ignition criterion become significant when B is around 10 and γ is >0.1, and Eq. (23) should be used.

It is worthwhile to point out that the value of γ is relative to the value of B in the case of the DPF. Ways to increase the value of γ are to increase the initial loading, decrease the wall thickness, or use materials with low heat capacity and density for the substrate wall. These techniques also increase the value of B. Thus, although Eq. (23) can predict more accurate results, the difference between Eqs. (23) and (25) is only 1–2 °C. Therefore, Eq. (25) is suitable for most DPF systems and operating conditions.

The analytical ignition criteria derived here can be used to help optimize the DPF system to obtain good fuel economy. Several design variables and operating parameters have been analyzed with the help of the analytical ignition criteria. The results of our analysis show that a thin channel wall, a high total filtration area, a high initial loading, a low gas flow rate and a high oxygen concentration are desirable for good fuel economy. However, the ignition criteria alone can not give the optimum result. The ignition criteria needs to be combined with the equations to predict ignition time, (which are reported in Zheng and Keith [4]), to optimize the DPF system.

Acknowledgement

The authors would like to thank the College of Engineering and Graduate School at MTU for financial support.

References

[1] J. Lahaye, P. Boehm, P. Chambrion, P. Ejrbirger, Combust. Flame 104 (1996) 199.

[2] R.W. McCabe, R.M. Sinkevitch, SAE Paper No. 860011 (1986).
[3] B. Stanmore, J.-F. Brilhac, P. Gilot, SAE Paper No. 1999-01-0115 (1999).
[4] H. Zheng, J.M. Keith, AIChE J. 50 (1) (2004) 184.
[5] V. Balakotaiah, D. Kodar, D. Nguyen, Chem. Eng. Sci. 50 (7) (1995) 1149.
[6] K. Ramanathan, V. Balakotaiah, D.H. West, Chem. Eng. Sci. 58 (8) (2003) 1381.
[7] D.T. Leighton, H.C. Chang, AIChE J. 41 (8) (1995) 1898.
[8] J.M. Keith, H.C. Chang, T. Leighton, AIChE J. 47 (3) (2001) 650.
[9] E.J. Bissett, F. Shadman, AIChE J. 31 (5) (1985) 753.
[10] J. Adler, J.W. Enig, Combust. Flame 8 (1964) 97.
[11] A.G. Konstandopoulos, J.H. Johnson, SAE Paper No. 890405 (1989).
[12] P. Versaevel, H. Colas, C. Rigaudeau, R. Noirot, SAE Paper No. 2000-01-477 (2000).
[13] O.K. Rice, A.O. Allen, H.C. Campbell, J. Am. Chem. Soc. 57 (1935) 2212.
[14] A.R. Shouman, A. El-Sayed, Combust. Flame 88 (1992) 321.
[15] K. Ogyu, A. Kudo, Y. Oshimi, SAE Paper No. 1003-01-0377 (2003).